

On the Dynamics of Mass Transfer with Chemical Reaction in Semi-batch Reactor

Kittiwat Wongpisan

Abstract

In this research, model for timewise semi-batch gas-liquid operation has been developed. In the approach of solving this problem, two NAG (Numerical Algorithms Group) Fortran Library Routines are needed: (1) D02EJF for integrating a system of time-varying ordinary differential equations (ODEs) using a variable-order, variable-step method implementing the Backward Differentiation Formulae (BDF); (2) C05AGF for iterating the local enhancement factor using a bisection method. With the aid of these solvers, the extents of film and bulk reaction at the different reaction rate constants can be quantified.

Keywords: semi-batch reactor, enhancement factor, chemical absorption, film and bulk reaction

1. Introduction

For the sake of simplification of gas-liquid reactor modeling and design, the reaction is usually assumed to be completed either entirely in the bulk of liquid or only within the liquid film. Nevertheless, an unwarranted restriction can also lead to serious pitfalls in the design.

Up to the present time, only some eight or so papers in gas-liquid absorption has been directed towards the analysis of intermediate reaction speed while the extensive literature on this area has been devoted to the reactions that are considered to be completely in the bulk of liquid or only within the liquid film [1]. None of these papers on the intermediate case deal with how the balance of film and bulk reaction is affected by the nature of the fluid mixing and type of gas-liquid contacting. Additionally, nowadays, general rate expressions for this intermediate regime (see Figure 1) are still unavailable [2].

This paper will outline an analysis of gas-liquid operation in a perfectly mixed semi-batch reactor to show how film and bulk reaction can be quantitatively computed for the general case at the different reaction rate constants.

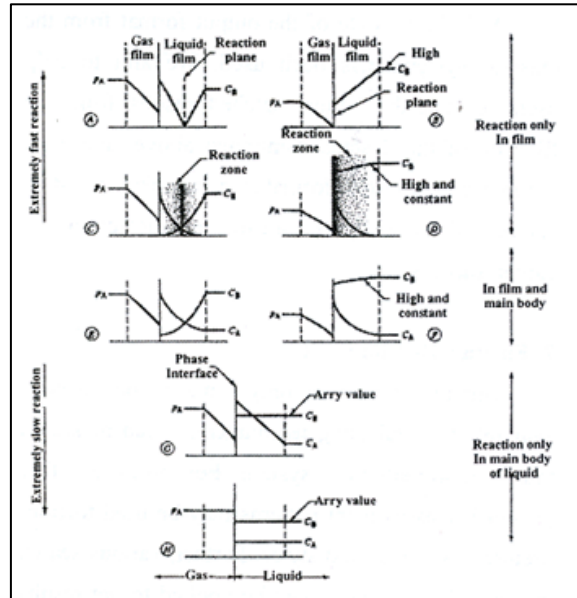


Figure 1 Interface behavior for the complete range of rates of reaction and mass transfer. Source: Levenspiel [2]

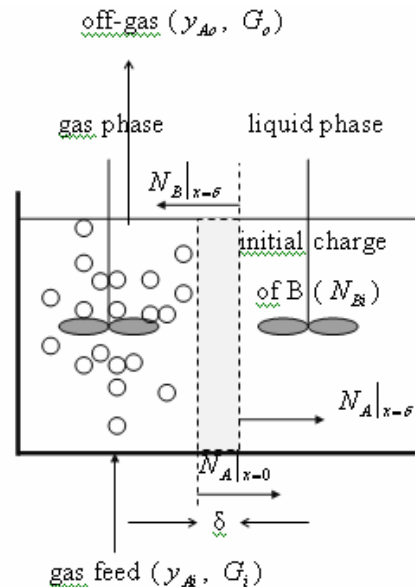


Figure 2 Schematic of perfectly mixed semi-batch reactor for 2nd order gas-liquid reaction, $A(g) + B(l) \xrightarrow{k_2} R(l)$

2. Model Formulation and Method of Solving

In a semi-batch gas-liquid reactor, species A (gas) is usually fed continuously through some sparging device at the bottom of the reactor while species B (liquid phase reactant) can be initially placed in the reactor (see Figure 2).

Two basic equations required to describe reactor performance are the material balance equation and the rate equation. A clear understanding of these basic equations and a willingness to write them down are essential. Considering Figure 2, if the reactor is perfectly spatially uniform, a material balance on any reactant species can be drawn up. It is as follows:

$$\begin{aligned} \text{Change of moles} &= \text{Moles entering element} + \\ \text{within element} &\quad \text{Moles leaving element} + \\ \left(\frac{dC_A}{dt}\right) &\quad \text{Moles reacting } (k_r C_{Abo} C_{Bbo} V) \end{aligned} \quad (1)$$

These four terms comprise the material balance. In a particular case, any one of the four terms in equation (1) may be zero. In this case, for example, the material balances on species A and B over the bulk of liquid phase are considered. Thus, the third term will be zero when the material balance on A over the liquid bulk is considered and the second term will be zero when the material balance on B over the liquid bulk is performed. To be able to calculate forth term, we must know the rate equation for the particular species. If this species is a reactant, its rate of reaction may depend upon the concentrations of several species, including its own. However, in this system, the reaction is considered to be second order (first order in both concentration of species A and B).

According to equation (1), the rate of change of concentration of A in the bulk of liquid phase during the operating time is equal to the flux of A from the film-bulk interface into the bulk of liquid minus the reaction rate between A and B in the bulk of liquid phase as shown in equation (2) while equation (3) shows the rate of change of concentration of B in the bulk of liquid phase which is equal to the amount of B placed in the reactor initially minus the flux of B from the film-bulk interface into the liquid film again minus the reaction rate between A and B in the bulk of liquid phase.

$$\frac{dC_{Abo}}{dt} = (N_A|_{x=\delta})/V - k_r C_{Abo} C_{Bbo} V \quad (2)$$

$$\frac{dC_{Bbo}}{dt} = N_{Bi} - (N_B|_{x=\delta})/V - k_r C_{Abo} C_{Bbo} V \quad (3)$$

The flux of reactant B at the gas film- bulk liquid interface ($N_B|_{x=\delta}$) must be equal by stoichiometry to the difference between the flux of reactant A at the gas-liquid interface and liquid-liquid film-bulk interface, as this represents the reactant A actually reacting in the film.

$$N_A|_{x=0} - N_A|_{x=\delta} = N_B|_{x=\delta} \quad (4)$$

Substituting equation (4) into equation (3) gives:

$$\frac{dC_{Bbo}}{dt} = N_{Bi} - (N_A|_{x=0} - N_A|_{x=\delta})/V - k_r C_{Abo} C_{Bbo} V \quad (5)$$

Referring to Danckwerts [3], the flux of reactant A from the gas-liquid interface into the liquid film ($N_A|_{x=0}$) and the flux from the liquid-film into the bulk of the liquid ($N_A|_{x=\delta}$) can be written as

$$N_A|_{x=0} = -D_A \left(\frac{dC_A}{dx}\right)_{x=0} \bar{V} a = k_L \bar{V} a \left(C_A^* - \frac{C_{Abo}}{\cosh \sqrt{M}}\right) E_A \quad (6)$$

$$N_A|_{x=\delta} = -D_A \left(\frac{dC_A}{dx}\right)_{x=\delta} \bar{V} a = k_L \bar{V} a \left(\frac{C_A^*}{\cosh \sqrt{M}} - C_{Abo}\right) E_A \quad (7)$$

where

$$E_A = \frac{\sqrt{\left(M \frac{E_i - E_A}{E_i - 1}\right)}}{\tanh \sqrt{\left(M \frac{E_i - E_A}{E_i - 1}\right)}} \quad (8)$$

$$M = \frac{D_A k_r C_{Bbo}}{k_L^2}$$

$$E_i = \left(1 + \frac{D_B C_{Bbo}}{z D_A C_A^*}\right)$$

To find the concentration of reactant A and B in the semi-batch perfectly stirred reactor at each moment during semi-batch operation is not simple. We can see that both equations (2 & 5) are ordinary differential equations which contain some unknown parameters, $N_A|_{x=0}$ and $N_A|_{x=\delta}$. If $N_A|_{x=0}$ and $N_A|_{x=\delta}$ are known, these two equations could be solved numerically by NAG Fortran Library Routine, for

example D02PCF, D02YAF or D02EJF (which are differential equation integrations).

D02PCF solves the initial value problem for a first order system of ordinary differential equations using Runge-Kutta method, while D02YAF integrates a system of first-order ordinary differential equations over one step, using Merson's Runge-Kutta method. D02EJF integrates a stiff system of first-order ordinary differential equations over an interval with suitable initial conditions, using a variable-order, variable-step method implementing the Backward Differential Formulae (BDF), until a user-specified function, if supplied, of the solution is zero. It then returns the solution at points specified by the user, if desired. In this work, after having tried to solve these equations by each of the three routines mentioned above, we chose routine D02EJF because this gave better efficiency over long ranges and for high accuracy computations compared to the previous two ones.

In order to obtain the value of $N_A \Big|_{x=0}$ and $N_A \Big|_{x=\delta}$, the enhancement factor has to be calculated first. Consider the material balance on reactant A over the gas phase in Figure 2, the rate of reactant A entering the gas phase is equal to the rate of reactant A leaving from the gas phase plus the flux of reactant A from the gas phase into the liquid-film interface as shown in the equation below.

$$G_i y_{Ai} = G_o y_{Ao} + N_A \Big|_{x=0} \quad (9)$$

where G_i and G_o are inlet and outlet gas molar flow rates, respectively. Rearranging equation (9) gives the rate of absorption of component A:

$$G_i y_{Ai} - G_o y_{Ao} = N_A \Big|_{x=0} \quad (9a)$$

Because there is no net change in the throughput of the inert gases,

$$G_i (1 - y_{Ai}) = G_o (1 - y_{Ao}) \quad (10)$$

Eliminating G_o by rearranging equation (10) and substituting into equation (9a) gives:

$$N_A \Big|_{x=0} = G_i \frac{(y_{Ai} - y_{Ao})}{(1 - y_{Ao})} \quad (11)$$

From Henry's law, the solubility relationship between the partial pressure of

component A (p_A) and the concentration of component A (C_A^*) at gas-liquid interface can be expressed by:

$$p_A = H_A C_A^* = y_{Ao} P \quad (12)$$

where H_A is Henry's constant, y_{Ao} is mole fraction of component A and P is the total pressure of the system.

Rearranging equation (12) for y_{Ao} , substituting into equation (11) and equating equation (11) with equation (6) gives:

$$k_L V \bar{a} (C_A^* - \frac{C_{Abo}}{\cosh \sqrt{M}}) E_A = G_i \left[\frac{(y_{Ai} - \frac{C_A^* H}{P})}{(1 - \frac{C_A^* H}{P})} \right] \quad (13)$$

Rearranging equation (13) gives a quadratic equation.

$$\begin{aligned} & \left(\frac{H}{P} V k_L \bar{a} E_A \right) C_A^{*2} - \\ & (V k_L \bar{a} E_A + \frac{H}{P} V \frac{k_L \bar{a} E_A C_{Abo}}{\cosh \sqrt{M}} + \frac{G_i H}{P}) C_A^* + \\ & (G_i y_{Ai} + \frac{V k_L \bar{a} E_A C_{Abo}}{\cosh \sqrt{M}}) = 0 \quad (14) \end{aligned}$$

This quadratic equation can be solved for C_A^* if the values of all parameters are given. In the step of solving at each instant of time during semi-batch operation, the value of C_{Abo} and C_{Bbo} will be given by the D02EJF solver (from NAG Fortran Library). These values will then be also used in the step of iteration of the enhancement factor at the same time. When C_A^* has been established, we can calculate the value of E_i . Then the enhancement factor can be calculated from equation (8)

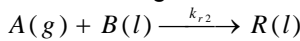
Because equation (8) is an implicit function, the enhancement factor should be solved for numerically. One of the routines in NAG Fortran Library document which can be used for this is C05AGF. C05AGF locates a simple zero of a continuous function from a given starting value, using a binary search to locate an interval containing a zero of the function, then a combination of the method of linear interpolation, extrapolation and bisection to locate the zero precisely.

In conclusion, in the whole program there are two NAG solvers: one for solving the ODEs

in the main program, another one (the subprogram) for iterating the local enhancement factor value. As realized before, the enhancement factor depends crucially on the concentration of reactant B in the bulk of the liquid. And now the concentration of B in bulk of liquid appears both in a system of ODE (equation 2 & 5) as well as in the enhancement factor. Thus these two NAG Fortran Library routines can solve for the answer simultaneously.

The solution algorithm for the reaction modeling of $A(g) + B(l) \xrightarrow{k_{r2}} R(l)$ when operated in semi-batch mode can be seen in Table 1. The following illustrative simulation (used the input parameters in Table 2) demonstrates the behavior of ozone reaction with organic substance for various reaction rate constants in a semi-batch reactor. These chemical and physical data are obtained from Perry and Green [4].

Table 1 Solution algorithm for the reaction



Unknowns	Equation number
C_A^*	(14)
y_{Ao}	(12)
G_o	(10)
C_{Abo}	Given by the D02EJF solver
C_{Bbo}	Given by the D02EJF solver
$N_A \Big _{x=0}$	(6), (9), (11)
$N_A \Big _{x=\delta}$	(7)
A&B reacted in liquid film	$N_A \Big _{x=0} - N_A \Big _{x=\delta}$
A&B reacted in liquid bulk	$k_r C_{Abo} C_{Bbo} V$
% saturation of A	$(C_{Abo} / C_A^*) * 100$
% absorption of A	$100 * (G_i y_{Ai} - G_o y_{Ao}) / G_i y_{Ai}$
% film reaction	$(\frac{\Delta N_A}{\Delta N_A + k_r V C_{Abo} C_{Bbo}}) * 100$

3. Results and Discussion

To demonstrate the behavior of ozone absorption and reaction in a semi-batch gas-liquid reactor, some of the simulated data have been plotted in the following figures. Figure 3 and Figure 4 show the effect of reaction rate constant on the liquid bulk concentration of reactant B (organic solute) and reactant A (ozone gas), respectively. The concentration of component B and A in the bulk of the liquid

decrease with an increase in the reaction rate constant. The higher value of reaction rate constant has a greater effect on both concentrations than the lower one.

Table 2 Parameters for reaction simulation,
 $A(g) + B(l) \xrightarrow{k_{r2}} R(l)$

Parameters	Values
D_A	$2.0 \times 10^{-9} \text{ m}^2 \text{ s}^{-1}$
D_B	$2.0 \times 10^{-9} \text{ m}^2 \text{ s}^{-1}$
a	$70 \text{ m}^2 \text{ m}^{-3}$
k_L	$2.1428 \times 10^{-5} \text{ m s}^{-1}$
H_A	$7.6 \times 10^6 \text{ N kmol}^{-1} \text{ m}^{-5}$
P	$1.01 \times 10^5 \text{ N m}^{-2}$
V	0.01 m^3
y_{Ai}	0.1
G_i	$1.0 \times 10^{-7} \text{ kmol s}^{-1}$
C_{Abo}	0 kmol m^{-3}
C_{Bbo}	$0.001 \text{ kmol m}^{-3}$
N_{Bi}	$1.0 \times 10^{-5} \text{ kmol}$
k_r	1, 5, 10, 50, 100, 500 $\text{m}^3 \text{ kmol}^{-1} \text{ s}^{-1}$

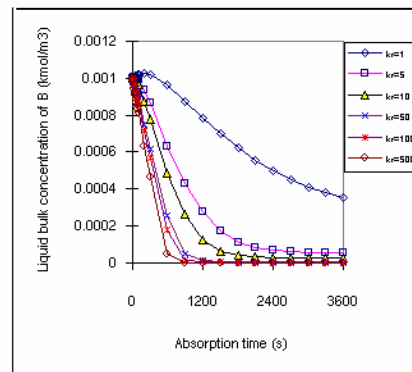


Figure 3 Depletion of liquid bulk concentration of reactant B at various reaction rate constants

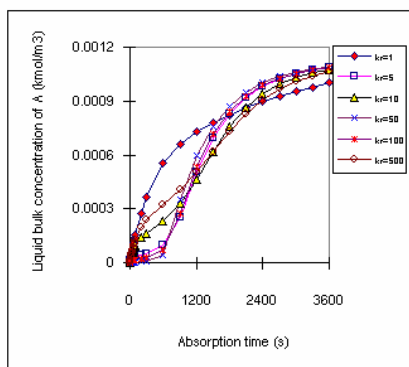


Figure 4 Change in liquid bulk concentration of component A during the illustrative semi-batch operating time

In addition, from these two figures, with an increase in absorption time, the liquid bulk concentration of reactant B and A changes inversely. The concentration of reactant B slowly decreases at the low reaction rate constant but rapidly decreases at the high reaction rate constant. At the beginning of semi-batch operation, the concentration of reactant A increases very quickly at the low reaction rate constant ($k_r = 1 \text{ m}^3 \text{ kmol}^{-1} \text{ s}^{-1}$) whilst at higher reaction rate constant these concentrations gradually increase and then begin to increase rapidly again after operating for 15-20 minutes.

In batch or semi-batch operation, the change of composition occurs in the time coordinate. Whether or not the operating system is uniform throughout its spatial co-ordinate, it always changes from moment to moment [5]. Several authors have been studying mass transfer with chemical reaction in batch and semi-batch operation. In the case of ozonation reaction, some experiments have also been conducted to investigate the behavior of ozone absorption and reaction in a semi-batch reactor, for example in the research work of Li and Kuo [6]; Baillod, Faith and Masi [7] and Dore et al. [8].

The inverse changes of concentration A (ozone) and B during the absorption time in semi-batch operation as mentioned above can be compared with the experimental research of Dore et al. [8]. Dore et al. investigated the absorption and ozonation of phenol in semi-batch reactor. During ozonation of phenol under semi-batch condition, the concentration of phenol and dissolved ozone in the bulk of liquid were also measured. The observed dissolved ozone and phenol concentration

during the absorption time is illustrated in Figure 5. The observed results indicate that it takes about 20 minutes for phenol of which the initial concentration is about 18 mg/l to vanish from the vessel before the build-up of dissolved ozone begins. Source: Dore et al. [8]

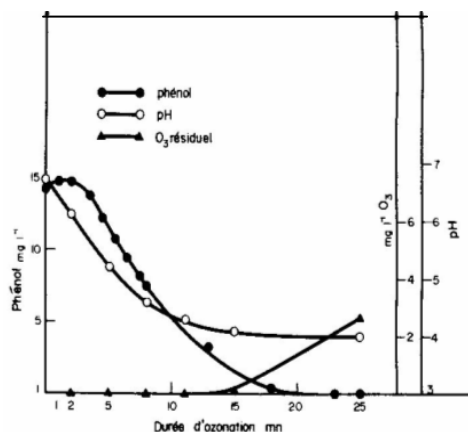


Figure 5 Observed ozone and phenol concentration during absorption time
 Source: Dore et al. [8]

Guroi [9] and Dietrich et al. [10] have observed that during ozonation of certain organic substances under semi-batch conditions, the concentration of dissolved ozone in the bulk of liquid phase remains undetectable until the concentration of organic substance decreases close to zero. According to the report of Mehta, George and Kuo [11], if a gas-liquid contactor is operated under semi-batch mode, the concentration of the organic compound declines with absorption time during the course of treatment while the enhancement factor may also decrease accordingly.

In this reaction simulation, the enhancement factor as well as the Hatta number is also calculated. Illustrated in Figure 6 and 7 are the enhancement factor and the Hatta number (Ha) plotted with the absorption time, respectively. Because of the great effect of the decrease in concentration of the liquid phase reactant B for the higher reaction rate constants, the enhancement factor decreases rapidly at the beginning of the semi-batch operation and then keeps stable till the end of the absorption time whilst for the low reaction rate constant, the enhancement factor is equal to one and stays constant till the end of the batch.

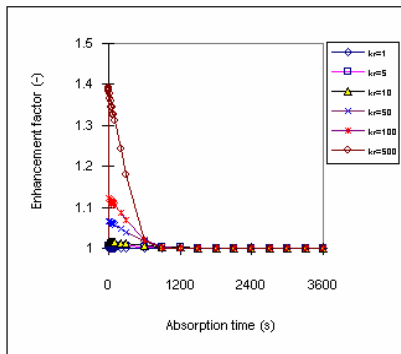


Figure 6 Effect of reaction rate constant on enhancement factor

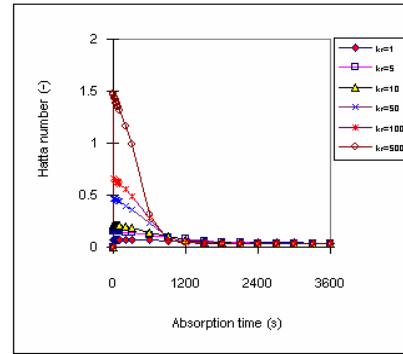


Figure 7 Effect of reaction rate constant on Hatta number

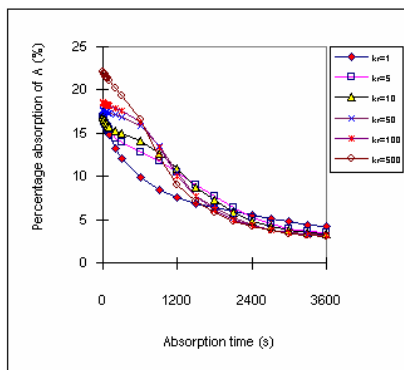


Figure 8 Percentage absorption at different reaction rate constants

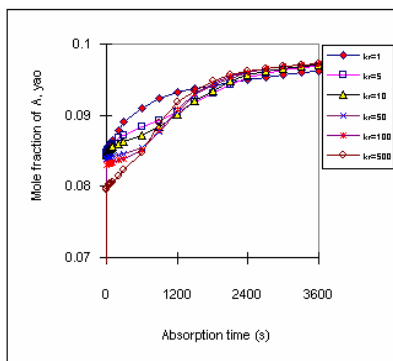


Figure 9 Change in mole fraction of A in gas Phase

Figure 8 shows the percentage absorption of reactant A at different values of reaction rate constants. This value is quite high at the beginning (16-22%) and low at the end of the absorption time (4-5%). This means that at the end of the treatment the amount of reactant A which is absorbed into the liquid is less than that at the beginning. This effect can be confirmed by Figure 9 which shows the change of mole fraction of reactant A in the exit gas

phase and Figure 10 which illustrates the increase in the total gas molar flow rate during the absorption time.

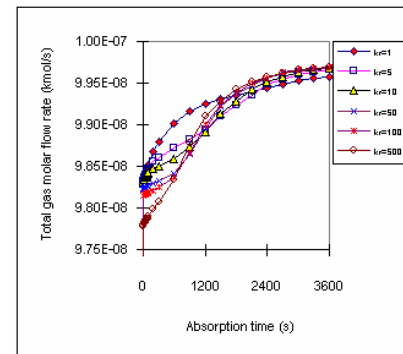


Figure 10 Total gas molar flow rate during absorption time

For all values of reaction rate constants, during the first half of the absorption time (see Figure 11), the reaction speed is high in comparison to that during the second half of the absorption time. This indicates that a large amount of reactant A diffuses through the gas-liquid interface and reacts with reactant B in the liquid phase causing a high value of percentage absorption of reactant A. Under this condition, there is not much unreacted reactant A in the gas bulk. Therefore, the values of mole fraction of A and total gas molar flow rate are low.

After the first half of the absorption time, the amount of reactant B which is initially placed in the reactor gradually decreases due to reacting with reactant A. During this period the reaction speed decreases. Less reactant A is consumed while gas A is still continuously fed into the vessel. Consequently, there is a huge amount of unreacted reactant A in the bulk of gas phase. We can see from Figure 9 and 10 that both mole fraction of reactant A and

total gas molar flow rate increase as the percentage absorption of A decreases during the absorption time.

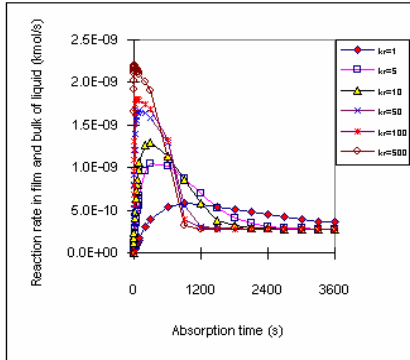


Figure 11 Reaction rates in both liquid film and liquid bulk

As described above, during the first half of the absorption time, the reaction speed is high. A large amount of reactant A is consumed by reacting with reactant B. Under this condition, there is not much unreacted reactant A at the gas-liquid interface (see Figure 12) or in the bulk of liquid (as seen earlier in Figure 4). On the other hand, the concentrations of gas A at the gas-liquid interface and in the liquid bulk increase again when the reaction speed gradually decreases till the end of the process. The relationship between the concentration of reactant A at the gas-liquid interface and in the liquid bulk is normally presented in terms of percentage saturation which is shown in Figure 13.

Moreover, during the first half of the absorption time, when the reaction rate constant increases, proportionally more of the reaction takes place in the liquid film (see the percentage film reaction in Figure 14). The amount of A and B reacted only in liquid film is depicted in Figure 15 while the amount of A and B reacted only in liquid bulk is also calculated and shown in Figure 16. Note that the summation of the amount of A and B reacted both in the liquid film and in the liquid bulk was presented earlier in Figure 11.

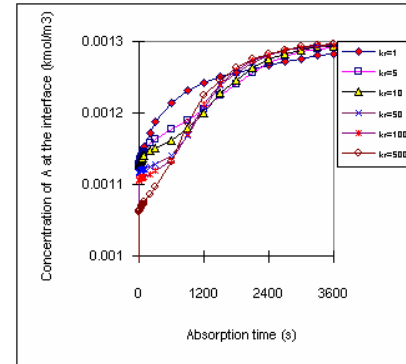


Figure 12 Change in concentration of reactant A at the gas-liquid interface

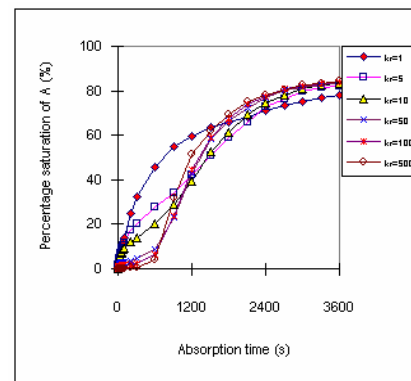


Figure 13 Change in percentage saturation of reactant A during semi-batch operation

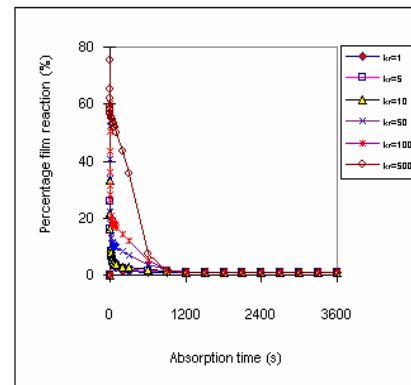


Figure 14 Effect of the reaction rate constant On the percentage film reaction

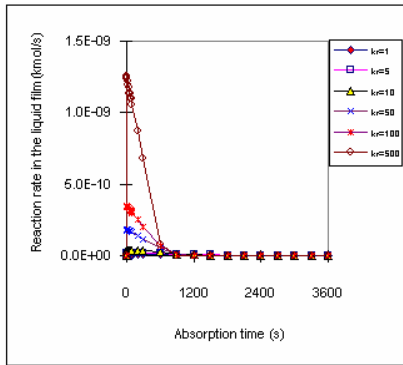


Figure 15 Reaction rates in liquid film during the process

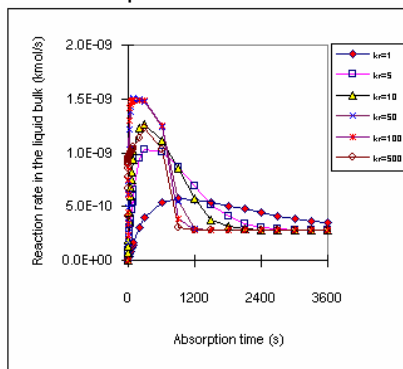


Figure 16 Reaction rate in liquid bulk during the process

One interesting aspect of this absorption which can be seen in these two Figures is the change in reaction location which is affected by the reaction speed. When the reaction speed is low, for example $k_r = 1 \text{ m}^3 \text{ kmol}^{-1} \text{ s}^{-1}$, all substrate A and B react in the bulk of liquid phase. None reacts in the liquid film. At a very high reaction rate constant, for example $k_r = 500 \text{ m}^3 \text{ kmol}^{-1} \text{ s}^{-1}$, the amount of substrate A and B reacted in the liquid film per unit time suddenly increases (see Figure 15) causing a high percentage film reaction as shown in Figure 14 whilst for the same reaction rate constant, this amount of substrate reacted in the bulk of liquid phase begins to decline (see Figure 16).

As seen in the simulated results presented, this model can predict not only the change of the reactants from the appropriate phases, but also how the relative amounts of film and bulk reaction vary in the liquid phase at the different reaction rate constants under semi-batch operation.

4. Conclusion

Without needing to impose either arbitrary diffusion-reaction regimes or film-bulk boundary conditions, a strategy has been devised for handling the proper calculation of film and bulk reaction in absorption with reaction in a gas-liquid semi-batch reactor. For a single perfectly mixed semi-batch reactor, two NAG Fortran Library Routines are used: one for solving a system of ODEs in the main program (D02EJF), another one (C05AGF, in the subprogram) for iterating the enhancement factor, since the enhancement factor depends crucially on the concentration of reactant B present in the bulk of the liquid phase. Now the concentration of B appears both in the system of ODEs as well as embedded in the enhancement factor. Thus, these two NAG Fortran Library routines can be solved simultaneously. Moreover, it can be seen that this model can predict not only the change of the reactants from the appropriate phases, but also how the relative amounts of film and bulk reaction vary in the liquid phase at the different reaction rate constants under semi-batch operation.

Nomenclature

\bar{a}	Interfacial area	$\text{m}^2 \text{ m}^{-3}$
A	Reactant A	
B	Reactant B (non-volatile substance)	
C_A	Concentration of reactant A	kmol m^{-3}
C_A^*	Concentration of A at gas-liquid interface	kmol m^{-3}
$C_{A_{bi}}$	Initial concentration of reactant A	kmol m^{-3}
$C_{A_{bo}}$	Liquid bulk concentration of reactant A	kmol m^{-3}
D_A	Diffusivity of reactant A	$\text{m}^2 \text{ s}^{-1}$
D_B	Diffusivity of reactant B	$\text{m}^2 \text{ s}^{-1}$
E_A	Enhancement factor, reaction factor	-
E_i	Enhancement factor for an infinitely fast reaction	-
G_i	Total gas molar flow rate (inlet)	kmol s^{-1}
G_o	Total gas molar flow rate (outlet)	kmol s^{-1}
Ha	Hatta number	-
H_A	Henry constant	$\text{N kmol}^{-1} \text{ m}^{-5}$

k_{r2}	Reaction rate constant for 2 nd order reaction	$\text{m}^3 \text{ kmol}^{-1} \text{ s}^{-1}$
k_L	Liquid side mass transfer coefficient	m s^{-1}
M	Film conversion parameter	-
$N_A _{x=0}$	Molar flow rate of A at gas-liquid interface	kmol s^{-1}
$N_A _{x=\delta}$	Molar flow rate of A at outer-liquid film interface	kmol s^{-1}
$N_B _{x=\delta}$	Molar flow rate of B at outer-liquid film interface	kmol s^{-1}
N_{Bi}	Amount of reactant B at the beginning	kmol
P	Total pressure of the system	N m^{-2}
p_A	Partial pressure	N m^{-2}
Q	Liquid volumetric flow rate	$\text{m}^3 \text{ s}^{-1}$
V	Liquid volume	m^3
y_{Ai}	Mole fraction of reactant A (inlet)	-
y_{Ao}	Mole fraction of reactant A (outlet)	-

References

1. Wongpisan, K. 2002. "Interactions of Mixing and Mass Transfer in Gas-Liquid Reactors", PhD thesis, UMIST.
2. Levenspiel, O. 1999. Chemical Reaction Engineering. 3rd ed., Wiley, New York.
3. Danckwerts, P.V. 1970. Gas-Liquid Reactions. McGraw-Hill, New York.
4. Perry, R.H. and Green, D.W. 1997. Perry's Chemical Engineers' Handbook. 7th ed., McGraw-Hill, U.S.A.
5. Denbigh, K.G. and Turner, J.C.R. 1984. Chemical Reactor Theory: An Introduction. Cambridge University Press, Cambridge, U.K.
6. Li, K.L. and Kuo, C.H. 1980. "Absorption and Reactions of Ozone in Phenolic Solutions", *AIChE Sym. Ser.*, 76, 161-170.
7. Baillod, C.R., Faith, B.M. and Masi, O. 1982. "Fate of Specific Pollutants During Wet Oxidation and Ozonation", *Envi. Prog.*, 1, 217- 226.
8. Dore, M., Langlais, B. and Legube, B. 1978. "Ozonation Des Phenols Et Des Acides Phenoxyacetiques" *Water Res.*, 12, 413-425.

9. Gurol, M.D. 1980. "Kinetic Behavior of Ozone in Aqueous Solution: Decomposition and Reaction with Phenol", Ph.D. Thesis, Univ. of North Carolina, Chapel Hill.
10. Dietrich, A.M., Chrostowski, P.C., Brunker, T.M. and Suffet, I.H. 1981. "Physical Chemical Mechanisms of Aqueous Ozonation", Paper presented at the A.S.C.E. National Conference on Environmental Engineering, Atlanta.
11. Mehta, Y.M., George, C.E. and Kuo, C.H. 1989. "Mass Transfer and Selectivity of Ozone Reactions", *Can. J. Chem. Eng.*, 67, 118-126.